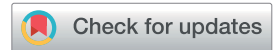
Environmental Science Processes & Impacts



PAPER

View Article Online
View Journal | View Issue



Cite this: Environ. Sci.: Processes Impacts, 2018, 20, 1559

Ice nucleation by particles containing long-chain fatty acids of relevance to freezing by sea spray aerosols†

Paul J. DeMott, * Ryan H. Mason, * Christina S. McCluskey, * Thomas C. J. Hill, * Russell J. Perkins, * Yury Desyaterik, * Allan K. Bertram, * Valeria Molinero, * Yuqing Qiu, * Valeria Molinero, * Yutaka Tobo, * Camille M. Sultana, * Christopher Lee * Allan K. Prather**

Heterogeneous ice nucleation in the atmosphere regulates cloud properties, such as phase (ice versus liquid) and lifetime. Aerosol particles of marine origin are relevant ice nucleating particle sources when marine aerosol layers are lifted over mountainous terrain and in higher latitude ocean boundary layers, distant from terrestrial aerosol sources. Among many particle compositions associated with ice nucleation by sea spray aerosols are highly saturated fatty acids. Previous studies have not demonstrated their ability to freeze dilute water droplets. This study investigates ice nucleation by monolayers at the surface of supercooled droplets and as crystalline particles at temperatures exceeding the threshold for homogeneous freezing. Results show the poor efficiency of long chain fatty acid (C16, C18) monolayers in templating freezing of pure water droplets and seawater subphase to temperatures of at least -30 °C, consistent with theory. This contrasts with freezing of fatty alcohols (C22 used here) at nearly 20 °C warmer. Evaporation of μL-sized droplets to promote structural compression of a C19 acid monolayer did not favor warmer ice formation of drops. Heterogeneous ice nucleation occurred for nL-sized droplets condensed on 5 to 100 µm crystalline particles of fatty acid (C12 to C20) at a range of temperatures below -28 °C. These experiments suggest that fatty acids nucleate ice at warmer than -36 °C only when the crystalline phase is present. Rough estimates of ice active site densities are consistent with those of marine aerosols, but require knowledge of the proportion of surface area comprised of fatty acids for application.

Received 23rd August 2018 Accepted 22nd October 2018

DOI: 10.1039/c8em00386f

rsc.li/espi

Environmental significance

Ice phase transitions in clouds over or near oceans may be triggered primarily by aerosol particles from oceanic emissions. While the specific particles or phases triggering ice formation remain poorly understood, their low efficiencies for freezing water can lead to deep cloud supercooling. Following the finding of long chain fatty acids as major components of some marine ice nucleating particles, this study explores their ice nucleation efficiencies and mechanisms. Fatty acids induced freezing when micron-sized solid particles were exposed to pure water at temperatures below $-28\,^{\circ}\text{C}$, varying non-monotonically by chain length. Freezing most likely occurred *via* particle surface defects rather than as monolayers. Studies to quantify the fatty acid size distribution in sea spray aerosols are needed to develop parameterizations from such work.

1 Introduction

Atmospheric ice nucleation plays a vital role in affecting the radiative properties of clouds below 0 °C and in triggering precipitation formation in clouds that are located in colder regions or extend to higher altitudes and lower temperatures. These are termed mixed-phase clouds, due to the coexistence of more deeply supercooled cloud droplets and heterogeneously nucleated ice crystals.¹ A variety of aerosols of natural and anthropogenic origin can be involved as atmospheric ice nucleating particles (INPs), including mineral and soil dusts, combustion particles, microbes and sea spray aerosol (SSA).² SSA INPs are distinct from land-sourced counterparts,

^aDepartment of Atmospheric Science, Colorado State University, Fort Collins, CO 80523-1371, USA. E-mail: Paul.Demott@colostate.edu

 $[^]bDepartment$ of Chemistry, University of British Columbia, Vancouver, British Columbia V6T 1Z1, Canada

^{&#}x27;National Center for Atmospheric Research, Boulder, CO 80307-3000, USA

^aLineberger Comprehensive Cancer Center, University of North Carolina, Chapel Hill, NC 27599. USA

^eDepartment of Chemistry and Biochemistry, University of California, San Diego, La Jolla, California 92093, USA

^fDepartment of Chemistry, The University of Utah, 315 South 1400 East, Salt Lake City, Utah, 24112-0550, USA

^gNational Institute of Polar Research, Tachikawa, Tokyo 190-8518, Japan

^hDepartment of Polar Science, School of Multidisciplinary Sciences, SOKENDAI (The Graduate University for Advanced Studies), Tachikawa, Tokyo 190-8518, Japan

 $[\]dagger$ Electronic supplementary information (ESI) available. See DOI: 10.1039/c8em00386f

especially in their limited emissions, which may make them less important over the continental middle-latitude regions of the Northern Hemisphere. However, they are of special importance at high latitudes and especially over the remote oceans of the Southern Hemisphere.3-6 In that region, their role in affecting anomalous cloud radiative properties in global climate model simulations (due to not being specifically differentiated) has been both proposed and supported by regional cloud model simulations using laboratory data on SSA INP properties.8 Nearer to some coastal mid-latitude regions in the Northern Hemisphere, INPs from oceans can importantly affect cloud properties when meteorology and topography combine to lead to the lifting of the marine boundary layer to form mixedphase clouds during the approach of winter storms. For example, along the west coast regions of North America, subtropical ocean moisture plumes referred to as "atmospheric rivers" are lifted over mountain ranges to drive heavy winter precipitation events that supply much of the annual water resources to the region.9 Direct impacts on altering cloud and precipitation processes occur in these cases, making it vitally important to understand the various sources of INPs within marine aerosols.10

Amongst INPs produced as components of SSA, diatoms and their exudates have been most commonly implicated as INP sources. An Inlie has led to attempts to specify their emissions in SSA through a one-to-one link between numbers present per organic matter in the sea surface microlayer and numbers expected per total predicted organic carbon mass emitted. This simple association has been questioned on the basis of laboratory mesocosm studies and atmospheric measurements. Aboratory studies instead indicate multivariate SSA INP compositions that are largely not specifically identified, but include dissolved and proteinaceous organic matter.

In the studies summarized by McCluskey *et al.*, ¹² one category of SSA INP compositions generated from separate experiments in a plunging water tank and a wave-breaking flume were particles of dominant compositions of long chain hydrocarbons. In different mesocosms, as described below, these long chain fatty acid-like particles could represent a range from 15 to 75% of INPs active at around $-30\,^{\circ}\text{C}$. Assessment could not be made of the contribution of these INP types at warmer temperatures due to experimental limitations, as also discussed below. We elaborate on these prior studies here because they essentially motivate the present set of more fundamental experiments on single compositions of particles.

The studies reported by McCluskey *et al.*¹² utilized real-time collection of INPs onto substrates after their activation to ice crystals in a continuous flow ice-thermal diffusion chamber. The INP composition of the dry residual particles remaining after evaporation of ice crystals were analyzed using micro-Raman spectroscopy, with reference spectra used for determining proportions of different types. INP spectra akin to a saturated fatty acid with composition of C16 (palmitic acid) were found for particles in the 1 μm size range in both experiments for activation conditions at $-30.5~^{\circ}C.^{12}$ Measurements in the same laboratory mesocosm studies have indicated the presence of surface active C8 to C24 fatty acids produced in SSA,

with palmitic acid and stearic acid (C18) comprising approximately two-thirds of the total ion signal of all tentatively identified saturated fatty acids.15 Long chain hydrocarbon INP compositions were most dominant (75% of INPs) during the death phase of a phytoplankton bloom induced in the plunging water tank experiments using wintertime ocean water collected at the Scripps Institution of Oceanography pier, for which Chl a concentration reached 40 μ g L⁻¹. This Chl a value is higher than commonly found in open oceans. For the lower Chl a (<5 $\mu g L^{-1}$) bloom induced in the wave-breaking flume of the Center for Aerosol Impacts on Chemistry of the Environment,16 INPs dominated by apparent long chain fatty acid compositions accounted for ~10-15% of total INP numbers released in SSA that were active via immersion freezing nucleation at near -30 °C.12 The role of saturated fatty acids at warmer cloud temperatures could not be assessed due to limitations on collecting a sufficient number of INPs for spectroscopic analysis, given the low number concentrations of INPs active.7 These results indicating that fatty acids were associated with ice nucleation were somewhat surprising due to few previous reports of the ability of such organic compounds to stimulate ice nucleation.11,17 Due to the surface-active nature of these compounds, ice nucleation could be imagined to be stimulated by monolayers on highly supercooled droplets, whereas the sizes and the high relative mass of particles found in the studies of McCluskey et al. 12 also merit consideration that these particles might nucleate ice as a crystalline phase when SSA takes up water in cold clouds.

It is necessary in this discussion to point out that we believe this class of INPs in SSA is distinct from the highly efficient ice nucleation entities found in the sea surface microlayer. ^{4,5} Although we cannot prove this point, it extends from two facts. First, the ice nucleating entities in these microlayer studies were active at small unit sizes, between 20 and 200 nm. Additionally, fatty acids would not be expected to be destroyed by thermal treatments to 100 °C. Heat lability was a specific feature of the microlayer ice nucleation entities reported by Wilson *et al.* ⁴ and Irish *et al.* ⁵ Heat lability and small INP sizes also characterize the majority of ice nucleating entities found in river waters, ^{18,19} which are thought to be of cell-free, fungal origin (*i.e.*, macromolecules, such as proteins ¹⁸). The possibility of fatty acid contributions to INP emissions from river regions has not been noted or yet explored.

No previous studies examining the ice nucleation behavior of crystalline carboxylic acids have been conducted, to our knowledge, except for the initial results on C16 from the set of experiments reported herein that were included in the recent study of Qiu *et al.*²⁰ Ice nucleation investigations of monolayers of carboxylic acids date to the time of first studies of the ice nucleation propensity of alcohol monolayers.^{21–23} It is by analogy to the templating action of alcohol monolayers that freezing of carboxylic acid monolayers is also imagined to occur, albeit with much lower efficiency. This has been investigated theoretically and *via* some first experiments by Qiu *et al.*²⁰ Freezing points by carboxylic acid monolayers in previous studies by Gavish *et al.*²¹ and Popovitz-Biro *et al.*^{22,23} were reported as controls on factors other than a difference in

structural match that affected freezing by homologous alcohol monolayers. These freezing points fell at a temperature just a few degrees warmer (at \sim -17 °C) than the freezing temperature of pure millimeter-sized (10 to 40 µL) water droplets on the hydrophobic surface of a cooled plate (-20 °C), and 18 °C warmer than the droplet homogeneous freezing temperature, with no dependence on C chain length. We might hypothesize that a source of insoluble contamination in the earlier studies was not identified, possibly coming from the chloroform used for monolayer spreading or the acid reagent itself. Alternately, some other aspect of the experimental design favored freezing at a condition a few degrees warmer than water droplets of the same basic purity. Average values for freezing temperatures of C16 (palmitic acid) monolayers on nanoliter droplets (see Section 2.1.1) were reported in Qiu et al.20 Freezing occurred at much lower temperatures and in better agreement with their predicted master freezing curve that has its basis in the lattice mismatch of the organic surfaces with ice. Supporting this are the results of Knopf and Forrester,11 who examined the freezing of nonadecanoic acid (C19) on water droplets in similar experiments, but using much smaller droplet sizes that cooled in a relatively pure state to as low as -29 °C before freezing. There was also no discernable influence on freezing of purified water droplets at these temperatures by C19 monolayers,11 consistent with predictions from Qiu et al.20 Furthermore, Knopf and Forrester¹¹ showed that the equilibrium spreading pressure is much lower on nonadecanoic acid than on the equivalent alcohol, nonadecanol, with the consequence that nonadecanoic acid monolayers exist in an expanded state at typical droplet surface pressures. Consistently lower spreading pressures for long chain fatty acids than alcohols have been reported elsewhere.24 Only when the subphase (below the surface monolayer) of drops is controlled to have higher salt (NaCl) concentrations does the equilibrium spreading pressure increase into the realm of a condensed phase monolayer structure. 11 Although ice nucleation was observed to occur for these latter conditions,11 freezing temperatures were still lower than for "pure" water due to the freezing point depression of the added salt.

One can imagine a similar situation for other long chain acids in this series besides C19. Lin et al.25 examined the structures of palmitic acid monolayers via molecular dynamics simulations with atomistic force fields. Although the head groups of C16 monolayers could take on hexagonal structures that begin to mimic those of ice, this occurs only at higher surface pressures, pressures that would not be expected under equilibrium conditions for pure water droplets. Again, higher surface pressures leading to less expanded structures might occur for more concentrated solutions, or perhaps under metastable conditions occurring during processes such as droplet evaporation. That is, during evaporation, the surface area per molecule will be reduced26 and surface pressure could be elevated above the typical equilibrium spreading pressure of long chain fatty acids. If a condensed phase is promoted, a more favorable structure for ice templating could occur. In this regard, we may note that the highest ice concentrations found in some tropical marine cumuli are in cloud regions where rapid evaporation of pre-existing liquid water droplets is

occurring,27 and the existence of evaporation-freezing nuclei during evaporation processes have been hypothesized, but never proven.28 While likely tied to secondary ice formation processes (ice "multiplication") known to occur in these clouds, it is useful to consider and explore all mechanisms that might link freezing to evaporation.

Nevertheless, any freezing scenario will be complicated by the complex compositional interaction in real SSA. In contrast to the pure surfactant films that are often studied, environmental films are likely to exist with many different surfactant components. The surfactants in these films are often miscible, which generally results in different structural organizations from those adopted for pure films, which consequently affects the ice nucleation activity of these films. Earlier studies support that when monolayer compositions are mixed, there is always a degradation of freezing ability.19 An exception to this trend would be if phase separation of one of the surfactants occurs, causing preservation of freezing ability. Another important type of interaction to consider in real systems is between soluble molecules, such as salts, and surfactants. Surfactants with acid groups will often coordinate with cations, changing their packing.29 While the packing conditions of the surfactant may become more favorable for freezing, the presence of the salt at the interface between the surfactant film and the water is expected to interfere with creating a surface that is structurally matched to ice, disrupting freezing.

In this study, we report on a range of experimental studies extending those reported in Qiu et al.,20 including studies of potential freezing of supercooled cloud droplets via the potential action of monolayers and crystalline particles of a range of chain lengths of long chain carboxylic acids. For monolayers, we also explore the roles of monolayer coverage, pH, and the potential impact of evaporation on freezing. A fatty alcohol is compared and contrasted as a positive control. The specific relevance of fatty alcohols within SSA via marine lipid sources is likely but unconfirmed. Fatty alcohols have been reported in the sea surface microlayer30,31 and in marine aerosols over remote regions via terrestrial sources that also deposit particles to the ocean surface.32,33 For studies of crystalline phases in contact with water, we examine freezing following condensation of small droplets onto substrate-deposited particles, and onto single, freely-suspended fatty acid particles.

Experimental 2

2.1 Freezing of drops as monolayers or in contact with crystalline fatty acid particles

A range of experimental studies were performed to explore freezing processes that could explain the association of long chain fatty acids with ice nucleation in SSA mesocosm studies. First, we used standardized procedures for placing bulk amounts of fatty acid and alcohols as monolayers on liquid droplets that are subsequently cooled toward freezing. We focused these monolayer studies on C16 and C18 carboxylic acids since these appeared as the most abundant in prior mesocosm studies. For a positive control, docosanol (C22H46O), previously identified as a very effective alcohol monolayer for freezing^{21,23} was used. These experiments were practically limited in detecting potential freezing by monolayers due to the macroscopic size of droplets needed for reliably distributing monolayer coverages. These microliter sizes in turn lead to a limit of supercooling before contaminants in purified water interrupt the experimental resolution of freezing by monolayers. We draw upon three separate, albeit similar device methods for these experiments in order to test consistency and to extend measurements to the lowest temperature possible. Nevertheless, most experiments are performed using only one of the methods (droplet freezing technique, DFT for shorthand) described below.

For C16 and C19 acids, we use a drop freezing device (ice spectrometer, IS for shorthand) that best permits exploring the role of evaporation on freezing of monolayers. These experiments are done for pure water subphase and filtered and diluted real SSA-containing droplets.

In order to extend studies to deeper supercooling than possible in microliter drops, approaching the homogeneous freezing temperature of pure water, we explore freezing of much smaller liquid drops condensed onto crystalline particle surfaces (alcohols and acids) with the DFT instrument. These latter experiments cover chain lengths from 12 to 20 for the carboxylic acids.

These various experiments and the different devices used in their conduct are described in this section.

2.1.1 University of British Columbia (UBC) droplet freezing technique (DFT). The DFT is a cold-stage flow cell device for observing ice nucleation for particles or droplets placed on a substrate.34,35 Following the procedure described by Popovitz-Biro et al., 23 ten to thirty 0.3-5 μL (800 to 2100 μm diameter) water droplets were pipetted onto a hydrophobic glass substrate (Hampton Research, Aliso Viejo, CA, USA) and then amended to add monolayers. Surfactants were added to the droplet using a CHCl₃ spreading solvent. In each experiment surfactant was not added to 2-3 droplets to act as an internal standard (CHCl₃ was added). After allowing for evaporation of the CHCl₃, alcohol or carboxylic acid surfactant concentration was calculated to estimate monolayer coverage in consideration of the exposed drop surface area on the substrates. Specifically, monolayer coverage was calculated in all cases by assuming 21 Å² per molecule and a hemispheric drop. The droplets were then placed in a temperature and humidity controlled flow cell coupled to an optical microscope. 20,34 The sample was cooled at a rate of 5 °C min⁻¹ until all droplets were frozen, as monitored by a video system. Based on a calculated characteristic time for thermal diffusion in water, the temperature at the center of the droplet will differ by less than 1 °C from the temperature at the surface of the droplet using this cooling rate for 5 μ L droplets. As additional variables in the experiments, partial and supermonolayer coverages and the role of droplet pH were investigated. Both ultrapure water and seawater were used as the subphase for droplets in different experiments. Operational temperature range for the size droplets used in these studies was 0 to -27 °C.

The DFT instrument was also used for crystalline phase freezing studies *via* first depositing particles onto the

hydrophobic glass substrates. Smaller droplets were formed on these particles via condensation, permitting studies to much lower freezing temperature, close to homogeneous freezing conditions for pure water droplets. Deposition of dry carboxylic acid particles was achieved by atomizing wet particles onto glass slides under clean conditions, and then drying the particles. Once crystalline particles were deposited (ESI, Fig. S1†), the sample was placed in the flow cell, and the water vapor pressure was adjusted to lead to condensation on the slide during cooling to near 0 °C. This led to the formation of 0.1 to 0.4 nL water droplets (60 to 90 µm diameter), whose freezing (presumably homogeneously) could be detected only at temperatures from -35 °C (10% frozen) to -36.5 °C (50% frozen). These droplets encapsulated from a few to a few tens of particles. Cooling at 5 °C min⁻¹ ensued following droplet formation, just as for the monolayer studies, and freezing of drops in contact with particles was monitored. It was expected that monolayers might also have formed on the droplet surfaces in this case, given the particle masses involved and the ability of a monolayer to form on an aqueous solution in contact with a crystal. We note that in Qiu et al.,20 this manner of experiment was interpreted as a monolayer freezing result for reporting a freezing condition of palmitic acid monolayers. Herein we compare and contrast the different flow cell experiments for a range of chain lengths. Additional comparison was provided by other ice nucleation instruments/experiments, as described below.

2.1.2 Colorado State University (CSU) ice spectrometer (IS). Droplet monolayer freezing studies were also conducted with the CSU IS.36,37 This instrument is usually operated using liquid aliquots, but for all present studies liquid droplets were placed on rectangular siliconized glass cover slides placed in thermal contact with the cooled aluminium blocks. For one set of experiments, 5 μ L droplets of deionized water (18 M Ω , 0.2 μ m filtered) were placed on each of four siliconized glass cover slides (22 × 22 mm, Hampton Research). Cover slides were placed on top of 1 mm thick glass slides that were attached to the face of the aluminium blocks, using thermal grease (Arctic Silver 5, Arctic Silver Inc.). To ten of these droplets, 0.5 μL of 50 mM palmitic acid (Sigma) dissolved in CHCl₃ (HPLC grade) was added and allowed to evaporate for 1 min to induce a thick multilayer coating. To the remaining 10 droplets, 0.5 µL of CHCl₃ was added. A microplate lid (Nunc) with holes cut in the sides and rear for ventilation was then placed over the coverslips, and HEPA-filtered N2 was supplied to prevent condensation within the sealed IS region. Cooling rate was -0.33 °C min⁻¹. Droplet freezing was assessed by visual inspection and imaging.

For studies of potential freezing during evaporation, 1 μL droplets were pipetted onto multiple 22 mm \times 22 mm siliconized cover slides (each attached to the block using several microliters of 66% glycerol in deionized water) and monolayers (0.25 μL of 0.25 mM acid, equating to two monolayers) were placed in the same manner as above. Varied array numbers (54 to 192 droplets), sub-phases (pure DI water, pure DI with NaCl added at 0.012% for concentration equivalency to a 1 μm cubic crystal dissolved into of a 25 μm supercooled cumulus cloud droplet, and collected SSA at a concentration equivalent again

to a dilute cloud droplet), two fatty acids as monolayers (palmitic and nonadecanoic), and temperatures from -19 to -23 °C were employed. The SSA sample was collected during experiments in a marine aerosol reference tank during January 2014.12 On the day of SSA collection, 326 L of SSA containing 5.6 mg m⁻³ aerosol by mass had been filtered through a 0.2 μm Nuclepore polycarbonate filter (Whatman), which was then resuspended in 5 mL deionized water to produce a 0.36 g L⁻¹ SSA solution (\sim 100-fold dilution of seawater, and 6 mM NaCl). This suspension was stored frozen until use in these experiments. The temperature range was chosen to be several degrees warmer than the lower instrument limit of -28 °C in order to limit freezing of negative controls and due to an expectation that if evaporation induced monolayer structural changes, these should make a large difference in the freezing temperature. Flow of N₂ was continued until the droplets became invisible to the eye, and only the monolayer residue could be seen if the droplet did not freeze first.

2.1.3 CRAFT (cryogenic refrigerator applied to freezing test). The CRAFT device is a cold plate device onto which a 7-by-7 array of droplets of 5 μ L volume are pipetted in an ultraclean chamber onto an aluminum surface coated with a thin layer of white petrolatum.38 The temperature of the plate is lowered at a rate of 1 °C min⁻¹, measured with an uncertainty of ± 0.2 °C. Freezing events are monitored by video to determine the number fractions of droplets frozen and unfrozen, recorded at 0.5 °C intervals. CRAFT can assess the freezing of pure water drops to close to the homogeneous freezing limit. Procedures for applying monolayers were the same as for other methods. Due to the possibility of contamination from the CHCl₃ or etching of the petrolatum layer, measurements are referenced to pure droplets with only CHCl3 added. Binomial confidence intervals (95%) were determined, as for the IS data, to establish uncertainties.

Single particle ice nucleation studies

A continuous flow diffusion chamber (CFDC)39 was used to examine freezing by freely-flowing (in air), pure palmitic acid particles in a limited set of experiments. The CFDC focuses particles into a central lamina, and ice-coated (cylindrical) wall temperatures are controlled to establish temperature and water relative humidity (RHw) conditions for the central aerosol particle lamina that is surrounded by particle-free sheath air. Setting relative humidity conditions to create water supersaturation ($SS_w = RH_w - 100\%$), promotes condensation to liquid droplets to a few µm in diameter. Residence time for freezing is \sim 5 seconds. Wall temperatures are adjusted in the outlet region of the device to promote evaporation of water droplets and wet aerosols, but ice particles continue to grow, and are counted optically at distinctly larger sizes (>4 µm) than other particles. At a certain value of SSw, liquid (unfrozen) droplets activated on aerosol particles grow large enough to survive through the evaporation zone, and this "water breakthrough" condition can be used to determine the total particle concentrations within the lamina.32 CFDC measurement uncertainties vary with processing conditions, and are typically $\pm 0.5~^{\circ}\text{C}$ and 2.4% water

relative humidity at -30 °C,39 the temperature where measurements were focused for this study. We follow Schill et al.40 for correcting sample concentrations for instrumental background (frost) and for defining confidence intervals for CFDC data.

Pure palmitic acid particles were aerosolized from a 0.25 mM solution of palmitic acid (PA) in methanol using a simple nebulizer. The aerosol generated by the nebulizer was not expected to resemble the bubble breaking mechanism associated with sea spray, and morphologically we could not know if the acid particles mimicked those generated in the reference tank experiments. Particles were size-selected at 100 nm using a differential mobility analyzer (Model 3081, TSI Inc.; sheath flow: 5 L min⁻¹, sample flow: 1 L min⁻¹). This size was selected primarily to optimize number densities for these studies. These particles were added to N2 flow and then counted using a condensation particle counter (CPC, TSI Model 3010, flow rate = 0.63 L min⁻¹), measured for chemical composition using an Aerodyne Research (Billerica, MA) aerosol mass spectrometer (AMS, flow rate = $0.09 L min^{-1}$ from 2.6 L min⁻¹ pumped flow), and assessed for ice nucleation using the CFDC (flow rate = 1.2L min⁻¹). Total PA particle concentrations were 1000 cm⁻³, and the AMS confirmed the particles contained palmitic acid, with unique mass to charge ratios (m/z) determined as m/z = 256, m/z= 129, and m/z = 213 (ESI, Fig. S2†). Particles were further dried in diffusion dryers prior to entry to the CFDC.

The phase state of particles after entry to the CFDC cannot be known for certain. Fitting water solubility with a second order polynomial and extrapolating to -30 °C suggests that only 5 picoliters of water are needed to dissolve the PA particles at this temperature. For the SS_w conditions used in the CFDC for this study, we calculate a minimum droplet diameter activated and grown in the CFDC of 3 $\mu m,^{39}$ giving a droplet volume of ${\sim}15$ picoliters. Thus, while the kinetics of dissolution cannot be resolved in the instrument, the equilibrium condition would be one of PA distributed to the droplet surface in an amount very close to a single monolayer within the growth region of the CFDC $(1.05 \times 10^6 \text{ molecules per 3 } \mu\text{m droplet, while a mono$ layer requires $\sim 1.41 \times 10^6$ molecules), transitioning to a multilayer coverage situation during evaporation. Thus, while we might assume that the CFDC experiments examine the occurrence of monolayer freezing at -30 °C, the timescale of the experiments is such that dissolution may not occur by the point of ice nucleation.

3 Results and discussion

Monolayer freezing study results

Fig. 1 shows 50% freezing condition results of all studies using the DFT, IS, and CRAFT instruments for which monolayers were placed using solutions in CHCl3. Most data are from the primary DFT experiments. Data are shown for docosanol, palmitic acid and stearic acid monolayers, as well as for the subphase only, whether pure water or seawater. Note that the subphase freezing temperature conditions shown are not the homogeneous freezing temperatures, but reflect the freezing nuclei content of purified water or filtered seawater and of the particular instrumental system (and surfaces) for assessing the

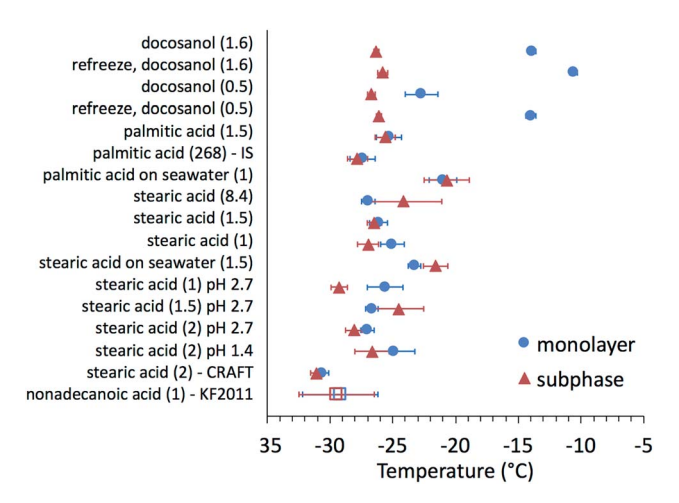


Fig. 1 Temperature at which 50% of 0.3 to 5 μ L droplets were observed to freeze, plus or minus 95% confidence intervals, when uncoated (subphase) or coated with monolayers (number of monolayers listed in parentheses). New results are shown primarily from the DFT device, except where specially noted for the CRAFT and IS. Docosanol was used as a positive control for subsequent experiments with palmitic acid, and stearic acid. The droplet subphase was pure water, except where seawater is noted. pH was adjusted in some stearic acid experiments. Results for nonadecanoic acid are as reported by Knopf and Forrester, 11 listed as KF2011 here. Results for docosanol (1.6) were reported previously by Qiu et al. 20

freezing of droplets up to 5 µL volume. The IS and DFT instruments have similar lower temperature limits for 5 µL droplets, but the CRAFT system was able to cool pure water droplets a few °C colder. Both 0.5 and 1.6 monolayers of docosanol were found to give freezing at temperatures significantly warmer in the DFT than for pure water droplets, and suggest that the methods were appropriate for placing monolayers. The lower freezing temperature of the 0.5 monolayer drops is consistent with the impact of sub-monolayer coverage on freezing found in prior studies.21 The experiment for calculated super-monolayer coverage (1.6 monolayers) is the same as discussed by Qiu et al.20 The freezing point of docosanol in this case is about 5 °C colder than reported in some other studies, 21,22 which may be partly explained by the use of droplets up to 10 times smaller in volume herein. Both 0.5 and 1.6 docosanol monolayer experiments also showed increased freezing temperature in second-freeze cycles, an expected behavior reflecting ice pre-activation of monolayer structures, as also reported in past studies. 41,42 These results give confidence to the subsequent measurements of acid monolayers.

In contrast to the alcohol, the differences in freezing temperature between coated and uncoated droplets using the long chain fatty acids as the surfactant were less than the uncertainty in the measurements in almost all cases (Fisher's exact test). In fact, the CRAFT system indicated no difference in freezing C18 acids to as low as $-30.7\,^{\circ}\text{C}.$ More experiments with larger monolayer coatings were also done with CRAFT, but the results are not shown because there was no change at all in freezing points. Previous results for nonadecanoic acid using a measurement system quite similar to the DFT (with 2 μL droplets) are included in Fig. 1.11 These are fully consistent with

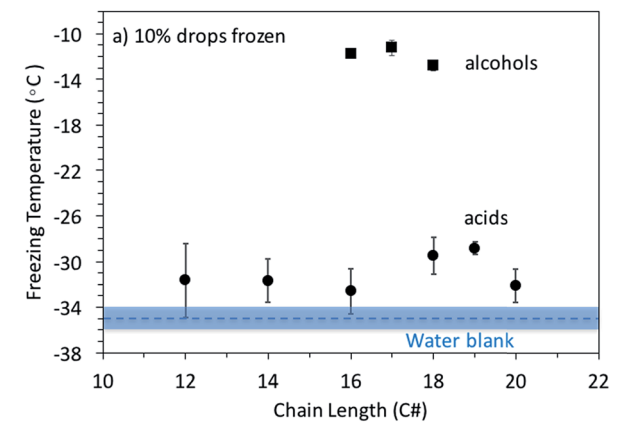
our results in showing no freezing impact of long chain fatty acid monolayers to temperatures of at least $-30\,^{\circ}$ C. In some DFT experiments, droplet pH was lowered for stearic acid to assure that no deprotonation of functional groups was occurring, since this could change the packing density of the monolayer. This step was simply a precaution, since the pK_a of stearic acid in a monolayer has been measured at $10.15.^{43}$ Freezing points remained essentially equal to the pure phase in the more acidic droplets, and systematic pH variations were not further explored.

3.2 Freezing of monolayer-coated droplets during evaporation

Experiments to explore evaporation-induced freezing of monolayer-coated droplets in the IS showed no positive response in any of the iterations performed. At approximately −19 °C, the diluted SSA sample without the monolayer recorded a single drop freezing event from 72 droplets without C16 added and no freezing droplets in an array of 54 with a C16 monolayer added, both observed over a 3.5 hour period. Results for a 192droplet array of diluted NaCl-containing droplets coated with a C19 monolayer and held at −23 °C are shown in ESI, Fig. S3.† No enhanced freezing compared to the control droplet array was observed over the course of that 4 hour experiment. While we cannot rule out that evaporation might restructure monolayers toward a configuration that favors freezing under some set of conditions, the results demonstrate that such an effect is not easily stimulated even at a few degrees warmer than where monolayers were not otherwise observed to freeze. In at least one case, the subphase was as ionically complex as could be expected in the ambient marine atmosphere (diluted SSA sample tested).

3.3 Results for freezing of crystalline fatty acids

In contrast to the monolayer studies of 0.3 to 5 µL droplets, freezing was reliably detected in many of the DFT experiments using solid particles, for which the freezing temperature could be lowered further toward homogeneous freezing conditions due to condensing much smaller droplets in contact with the particles. Fig. 2 shows the 10% and 50% frozen percentages of nL droplets freezing for C12 to C20 straight-chain carboxylic acids and C16-C18 straight-chain alcohols. These document an approximately 1 to 2 °C decrease in temperature when frozen percentage increases from 10 to 50% for the alcohols. All of these have 50% freezing temperatures between -12.8 and -14.1 °C, comparable to values previously reported for monolayers.21,23 The fatty acids all have 10% freezing temperatures significantly warmer than the water blanks. No monotonic chain length relation is noted. Instead, stearic acid (C18) and nonadecanoic acid (C19) stand out as significantly more efficient for heterogeneous ice nucleation. This same pattern is repeated for the 50% freezing temperatures, with C18 and C19 acids freezing warmest, at approximately -33.7 °C and −30.6 °C, respectively (Table S1, ESI†). At this freezing condition, C14 and C20 acids are indistinguishable from the water blank. Transition from 10 to 50% freezing conditions occurred



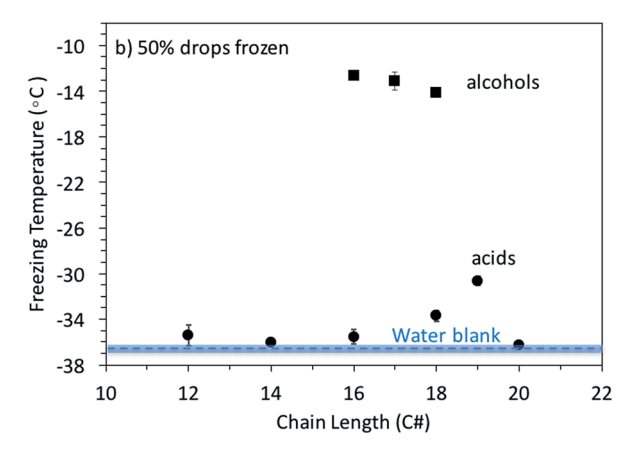


Fig. 2 The average freezing temperature and 95% confidence interval at which 10% (panel a) and 50% (panel b) of droplets containing or in contact with particles of the specified carboxylic acid of given chain length number froze. Also included is the average freezing temperature (dashed line) and 95% confidence interval (shaded region) of ultrapure water droplets. Results for 50% freezing of drops on C16 were used previously as the basis for the warmest freezing temperature of monolayers by Qiu et al.20

with about a 4 °C decrease in temperature for most of the fatty acids, but was only 1.8 °C for C19 (Table S1, ESI†).

There are two possibilities for explaining the fact that freezing was observed for crystalline phase particles and not for monolayers. Because all 10% and 50% freezing temperatures in Fig. 2 are lower than any of the conditions achieved for monolayer experiments, and because monolayers would be expected to occur in the nL experiments via spreading of the surfactant on the water droplets during the few minutes of cooling in the DFT, it is reasonable to consider that these experiments were able to achieve the freezing conditions for monolayers.20 However, we have no explanation for why C18 and especially C19 would be favoured for monolayer freezing. The expectation based on theoretical considerations is that the freezing efficiency would monotonically increase over chain length in the range covered.20 Alternately, it is also possible that the larger crystalline particles contain defects or active sites capable of initiating heterogeneous freezing. This is unexpected on the basis of templating considerations discussed by Qiu et al.20

Reasons why carboxylic acids might freeze in this manner, and why C19 might be most favoured for such, remain for future research consideration.

CFDC measurements of palmitic acid freezing

Insight into the mechanism for freezing was sought through the experiments generating a continuous flow of 100 nm pure palmitic acid particles for sampling by the CFDC instrument. An experimental timeline is shown in Fig. S4.† Particles were initially processed at relatively high water supersaturation (SS_w \sim 8%) to promote complete condensation of water onto particles to form cloud droplets prior to any subsequent freezing. The processing temperature was -30.5 ± 0.5 °C in order to be equivalent to the studies of McCluskey et al. for which fatty acid particles were detected as residuals of ice nucleating particles.12 A period of PA sampling was bookended by two periods to establish instrument background. The SS_w of particle exposure was then raised above 15% to cause liquid droplets to be detected surviving through the evaporation section of the CFDC in order to validate that the concentration of total particles within the instrument was equal to the number measured upstream (i.e., no measurable particle losses occurred). Freezing of a small fraction of PA particles was inferred, albeit not at a level of significance above background. INP concentrations were $0.92 \pm 0.98~\mathrm{L^{-1}}$ from a sampled concentration of 1000 cm⁻³. Hence, the maximum fraction freezing was 1 in 10⁶ particles. This may be compared to 20 freezing in 10⁶ total particles when sampling SSA in the seawater mesocosm from which PA-like particles were detected as ice crystal residual nuclei12 (see Fig. S5†).

As discussed in Section 2, the phase state of the particles in the current experiments could not be verified. Even though dissolution and formation of a monolayer was possible, we do not know if sufficient time was available in the CFDC growth region for this to occur. Partial dissolution would mean that the experiments were examining freezing by solid particles, albeit of surface area up to 100 times smaller than the fatty acid particles detected by McCluskey et al.12 as residuals of nucleated ice crystals. This could also explain the lower apparent freezing efficiency (see next section).

Although one might wish to conduct further experiments with larger PA particles that would assuredly remain largely non-dissolved, to be more equivalent to the mesocosm observations, a key point is that these experiments support a requirement that a substantial mass of particulate fatty acids must be present in larger SSA particles in order for these to be associated at all with freezing at temperatures up to several degrees warmer than the homogeneous freezing limit.

Fatty acids and freezing of sea spray aerosols

We briefly consider here the implications of results for freezing of SSA due to their content of fatty acids. The C16, and C18 results are most relevant in this regard based on their relative abundance in SSA,14 while the more active C19 is not relevant. Any such discussion of implications is of course somewhat speculative due to the lack of needed quantitative information on representative numbers of natural SSA containing fatty acids, and their mass or surface area distribution. If the freezing data on crystalline fatty acids is interpreted to represent monolayer freezing, then the master freezing curve approach of Qiu $et\ al.^{20}$ could be used to develop a freezing rate parameterization for atmospheric models. A rapid freezing process would be expected to ensue in proximity to the homogeneous freezing temperature for all cloud droplets formed on SSA particles and containing sufficient mass of carboxylic acids. Based on the experimental observations, freezing rates would decrease an order of magnitude per 4 to 5 °C.

If we presume that the CFDC and DFT measurements represent heterogeneous freezing of features on the crystalline particle surfaces, we may calculate the freezing number per surface area in experiments, to estimate the active site density³⁶ (referred to as n_s , with unit cm⁻²). This parameter is derived under approximating freezing as a deterministic process. If we assume spherical particles, a geometric $n_{s,geo}$ value of 3183 cm⁻² is determined from the CFDC measurements on 100 nm palmitic acid particles at -30.5 °C (assuming little dissolution). As for INP number in that experiment, there is no statistical significance to this determination. In the plunging water mesocosm experiment of McCluskey et al.,12 long chain fatty acids were present as a major component of \sim 18% of particles in the submicron diameter range. Using this as a maximum estimate for the ratio of total SSA surface area to associate with the measured INP number concentrations (see Fig. S5† for these values) attributed to fatty acids, we infer a minimum $n_{\rm s,geo}$ of 8961 cm⁻² at -30.5 °C. These values may be compared to a value of 4558 cm⁻² calculated from a parameterization developed for marine aerosols on the basis of atmospheric measurements.14 Finally, we may estimate the geometric surface area of stearic acid in the DFT experiment shown in Fig. S4.† Poor knowledge of their three-dimensional structure provides the largest uncertainty, which could be up to an order of magnitude. As a crude approximation for these non-spherical particles, we assume a total exposed surface areas of half of their circumscribed spherical diameters. Since these calculations are demonstrative only, we ignore summing freezing events by particle size, but instead use the total estimated surface area of 1.6×10^{-3} cm² covered by all drops in the field of view for estimating $n_{\rm s,geo}$. Values of 1241 cm⁻² and 6206 cm⁻² are determined for C18 at -29.7 and -33.7 °C, respectively. These values compare to values of 2643 cm⁻² and 26 073 cm⁻² predicted by the McCluskey et al.14 parameterization for marine INPs. These estimates suggest a significant contribution by fatty acids at these temperatures that would be in proportion to the ratio of the fatty acid to total particle surface area. Again, this latter information is not known. Finally, we may note that the frozen fraction change per temperature in our studies (~1 order of magnitude per 4 to 5 °C) is similar to that found for natural marine aerosols,14 suggesting that it is at least possible that fatty acids could contribute in some proportion as SSA INPs not only at the lower temperatures investigated in this study, but at other mixed-phase cloud temperatures.

4 Conclusions

Experiments were performed to seek to explain the observation from laboratory mesocosm experiments that long chain fatty acid particles within SSA particles participate in ice nucleation at temperatures at near and below -30 °C, as summarized in ESI (Table S1).† Confirmation was obtained from a series of experiments in which larger (supermicron to 100 μm) solid particles of straight chain carboxylic acids (C12-C20) were made to be in contact with pure water droplets of 60 to 90 µm average diameters. Stearic and nonadecanoic acid were the most efficient at freezing drops. That this occurs for one of the most abundant such acids found in SSA (C18) validates the relevance of such particles for freezing in the mixed-phase cloud regime. The mechanism for freezing could not be confirmed, but appears to be heterogeneous nucleation induced by properties of the crystalline surfaces, since no experiments clearly validated freezing of monolayers as the primary mechanism. Specifically placing monolayers on mmsized drops did not lead to a distinct difference in the freezing temperature in comparison to pure droplets or droplets of seawater. This process was tested in three different devices capable of studies to a limit of about -30.7 °C prior to 50% freezing. Unfortunately, none of these experiments could achieve a detection temperature as low as observed for the same long chain fatty acids in the crystalline particle experiments. An attempt to freeze pure palmitic acid particles without a substrate, within the CFDC instrument, showed an extremely low fraction freezing, amounting to 1 in a million particles, one hundred times less efficient than observed for long chain acid-like particles in mesocosm studies at -30.5 °C and far lower than the 10% freezing fraction observed for nL droplets in contact with crystalline palmitic acid. While this experiment was conducted for activated droplet sizes that should have resulted in monolayer coverages, thus supporting that freezing by the crystalline surface is the primary mechanism at play, it is also possible that the 100 nm particles remained only partially dissolved in the CFDC studies. Thus, while the results herein appear to most strongly support nucleation by some characteristic of non-dissolved fatty acid surfaces, unlikely based on bulk structure,20 the inability to resolve the explicit mechanism does not minimize the overarching result that the freezing ability of these types of substances within SSA is likely, at least under deep supercooling in clouds. The calculation of active site density parameters on the assumption of freezing by solid fatty acid surfaces that are of the same order as those measured for marine INPs confirms their potential role in freezing at below about -30 °C. The temperature dependence of freezing in the DFT experiments of solid fatty acids suggests a process that may contribute SSA INPs over an even broader temperature range of mixed-phase clouds.

Conflicts of interest

There are no conflicts to declare.

Acknowledgements

This work was supported by the U.S. National Science Foundation (NSF) through the NSF Center for Aerosol Impacts on Chemistry of the Environment (CAICE), CHE-1801971. A. K. Bertram and R. H. Mason acknowledge support from the Natural Sciences and Engineering Research Council of Canada. Y. Tobo acknowledges support from ISPS KAKENHI Grant Numbers 15K13570, 16H06020, and 18H04143. Kotaro Murata is acknowledged for technical support of CRAFT measurements. Misha Schurman is acknowledged for assistance with setting up Aerosol Mass Spectrometer measurements.

Notes and references

- 1 U. Lohmann and J. Feichter, Global indirect aerosol effects: a review, Atmos. Chem. Phys., 2005, 5, 715-737.
- 2 Z. A. Kanji, L. A. Ladino, H. Wex, Y. Boose, M. Burkert-Kohn, D. J. Cziczo and M. Krämer, Overview of Ice Nucleating Particles, Meteorol. Monogr., 2017, 58, 1.1-1.33, DOI: 10.1175/AMSMONOGRAPHS-D-16-0006.1.
- 3 S. M. Burrows, C. Hoose, U. Pöschl and M. G. Lawrence, Ice nuclei in marine air: Biogenic particles or dust?, Atmos. Chem. Phys., 2013, 13, 245-267, DOI: 10.5194/acp-13-245-2013.
- 4 T. W. Wilson, L. A. Ladino, P. A. Alpert, M. N. Breckels, I. M. Brooks, J. Browse, S. M. Burrows, K. S. Carslaw, J. A. Huffman, C. Judd, W. P. Kilthau, R. H. Mason, G. McFiggans, L. A. Miller, J. J. Nájera, E. Polishchuk, S. Rae, C. L. Schiller, M. Si, J. Vergara Temprado, T. F. Whale, J. P. S. Wong, O. Wurl, J. D. Yakobi-Hancock, J. P. D. Abbatt, J. Y. Aller, A. K. Bertram, D. A. Knopf and B. J. Murray, A marine biogenic source of atmospheric icenucleating particles, Nature, 2017, 525, 234-238, DOI: 10.1038/nature14986.
- 5 V. E. Irish, S. Hanna, Y. Xi, M. Boyer, E. Polishchuk, J. Chen, J. P. D. Abbatt, M. Gosselin, R. Chang, L. Miller and A. K. Bertram, Revisiting properties and concentrations of ice nucleating particles in the sea surface microlayer and bulk seawater in the Canadian Arctic during summer, Atmos. Chem. Phys. Discuss., 2018, DOI: 10.5194/acp-2018-641, in review.
- 6 J. Vergara-Temprado, B. J. Murray, T. W. Wilson, D. O'Sullivan, J. Browse, K. J. Pringle, K. Ardon-Dryer, A. K. Bertram, S. M. Burrows, D. Ceburnis, P. J. DeMott, R. H. Mason, C. D. O'Dowd, M. Rinaldi and K. S. Carslaw, Contribution of feldspar and marine organic aerosols to global ice nucleating particle concentrations, Atmos. Chem. Phys., 2017, 17, 3637–3658, DOI: 10.5194/acp-17-3637-2017.
- 7 P. J. DeMott, T. C. J. Hill, C. S. McCluskey, K. A. Prather, D. B. Collins, R. C. Sullivan, M. J. Ruppel, R. H. Mason, V. E. Irish, T. Lee, C. Y. Hwang, T. S. Rhee, J. R. Snider, McMeeking, S. Dhaniyala, E. R. J. J. B. Wentzell, J. Abbatt, C. Lee, C. M. Sultana, A. P. Ault, J. L. Axson, M. Diaz Martinez, I. Venero, G. Santos-Figueroa, M. D. Stokes, G. B. Deane, O. L. Mayol-Bracero, V. H. Grassian, T. H. Bertram, A. K. Bertram, B. F. Moffett

- and G. D. Franc, Sea spray aerosol as a unique source of ice nucleating particles, Proc. Natl. Acad. Sci. U. S. A., 2016, 113(21), 5797-5803, DOI: 10.1073/pnas.1514034112.
- 8 J. Vergara-Temprado, A. K. Miltenberger, K. Furtado, D. P. Grosvenor, B. J. Shipway, A. A. Hill, J. M. Wilkinson, P. R. Field, B. J. Murray and K. S. Carslaw, Strong control of Southern Ocean cloud reflectivity by ice-nucleating particles, Proc. Natl. Acad. Sci. U. S. A., 2018, 115(11), 2687-2692, DOI: 10.1073/pnas.1721627115.
- 9 P. J. Neiman, M. Hughes, B. J. Moore, F. M. Ralph and E. M. Sukovich, Sierra Barrier Jets, Atmospheric Rivers, and Precipitation Characteristics in Northern California: A Composite Perspective Based on a Network of Wind Profilers, Mon. Weather Rev., 2013, 141, 4211-4233, DOI: 10.1175/MWR-D-13-00112.1.
- 10 D. Rosenfeld, R. Chemke, P. J. DeMott, R. C. Sullivan, R. Rasmussen, F. McDonough, J. Comstock, B. Schmid, J. Tomlinson, H. Jonsson, K. Suski and K. Prather, The Common Occurrence of Highly Supercooled Drizzle and Rain near the Coastal Regions of the Western United States, J. Geophys. Res.: Atmos., 2013, 118, 9819-9833, DOI: 10.1002/jgrd.50529.
- 11 D. A. Knopf and S. M. Forrester, Freezing of Water and Aqueous NaCl Droplets Coated by Organic Monolayers as a Function of Surfactant Properties and Water Activity, J. Phys. Chem. A, 2011, 115, 5579-5591, DOI: 10.1021/ jp2014644.
- 12 C. S. McCluskey, T. C. J. Hill, C. M. Sultana, O. Laskina, J. Trueblood, M. V. Santander, C. M. Beall, J. M. Michaud, S. M. Kreidenweis, K. A. Prather, V. H. Grassian and P. J. DeMott, A mesocosm double feature: Insights into the chemical make-up of marine ice nucleating particles, J. Atmos. Sci., 2018a, 75, 2405-2423, DOI: 10.1175/JAS-D-17-0155.1.
- 13 C. S. McCluskey, T. C. J. Hill, F. Malfatti, C. M. Sultana, C. Lee, M. V. Santander, C. M. Beall, K. A. Moore, G. C. Cornwell, D. B. Collins, K. A. Prather, K. Jayarathne, E. Stone, F. Azam, S. M. Kreidenweis and P. J. DeMott, A dynamic link between ice nucleating particles released in nascent sea spray aerosol and oceanic biological activity during two mesocosm experiments, J. Atmos. Sci., 2017, 74, 151-166, DOI: 10.1175/JAS-D-16-0087.1.
- 14 C. S. McCluskey, J. Ovadnevaite, M. Rinaldi, J. Atkinson, F. Belosi, D. Ceburnis, S. Marullo, T. C. J. Hill, U. Lohmann, Z. A. Kanji, C. O'Dowd, S. M. Kreidenweis and P. J. DeMott, Marine and Terrestrial Organic Ice Nucleating Particles in Pristine Marine to Continentally-Influenced Northeast Atlantic Air Masses, J. Geophys. Res.: Atmos., 2018b, 123, 6196-6212, DOI: 10.1029/ 2017JD028033.
- 15 R. E. Cochran, O. Laskina, T. Jayarathne, A. Laskin, J. Laskin, P. Lin, C. Sultana, C. Lee, K. A. Moore, C. D. Cappa, T. H. Bertram, K. A. Prather, V. H. Grassian and E. A. Stone, Analysis of organic anionic surfactants in fine and coarse fractions of freshly emitted sea spray aerosol, Environ. Sci. Technol., 2016, 50, 2477-2486, DOI: 10.1021/ acs.est.5b04053.

- 16 K. A. Prather, T. H. Bertram, V. H. Grassian, G. B. Deane, M. D. Stokes, P. J. DeMott, L. I. Aluwihare, B. Palenik, F. Azam, J. H. Seinfeld, R. C. Moffet, M. J. Molina, C. D. Cappa, F. M. Geiger, G. C. Roberts, L. M. Russell, A. P. Ault, J. Baltrusaitis, D. B. Collins, C. E. Corrigan, L. A. Cuadra-Rodriguez, C. J. Ebben, S. D. Forestieri, T. L. Guasco, S. P. Hersey, M. J. Kim, W. Lambert, R. L. Modini, W. Mui, B. E. Pedler, M. J. Ruppel, O. S. Ryder, N. Schoepp, R. C. Sullivan and D. Zhao, Bringing the ocean into the laboratory to probe the chemical complexity of sea spray aerosol, *Proc. Natl. Acad. Sci. U. S. A.*, 2013, 110(19), 7550–7555, DOI: 10.1073/pnas.1300262110.
- 17 D. A. Knopf, P. A. Alpert and B. Wang, The Role of Organic Aerosol in Atmospheric Ice Nucleation: A Review, *ACS Earth Space Chem.*, 2018, 2(3), 168–202, DOI: 10.1021/acsearthspacechem.7b00120.
- 18 K. A. Knackstedt, B. F. Moffett, S. Hartmann, H. Wex, T. C. J. Hill, E. D. Glasgo, L. A. Reitz, S. Augustin-Bauditz, B. F. N. Beall, G. S. Bullerjahn, J. Fröhlich-Nowoisky, S. Grawe, J. Lubitz, F. Stratmann and R. M. L. McKay, Terrestrial Origin for Abundant Riverine Nanoscale Ice-Nucleating Particles, *Environ. Sci. Technol.*, 2018, DOI: 10.1021/acs.est.8b03881.
- 19 B. F. Moffett, T. C. J. Hill and P. J. DeMott, Abundance of Biological Ice Nucleating Particles in the Mississippi and Its Major Tributaries, *Atmosphere*, 2018, 9, 307, DOI: 10.3390/atmos9080307.
- 20 Y. Qiu, N. Odendahl, A. Hudait, R. H. Mason, A. K. Bertram, F. Paesani, P. J. DeMott and V. Molinero, Ice nucleation efficiency of hydroxylated organic surfaces is controlled by their structural fluctuations and mismatch to ice, *J. Am. Chem. Soc.*, 2017, 139, 3052–3064, DOI: 10.1021/jacs.6b12210.
- 21 M. Gavish, R. Popovitz-Biro, M. Lahav and L. Leiserowitz, Ice Nucleation by Alcohols Arranged in Monolayers at the Surface of Water Drops, *Science*, 1990, **250**, 973–975.
- 22 R. Popovitz-Biro, M. Lahav and L. Leiserowitz, Ice Nucleation: A Test to Probe the Packing of Amphiphilic Alcohols at the Oil-Water Interface, *J. Am. Chem. Soc.*, 1991, **113**, 8943–8944.
- 23 R. Popovitz-Biro, J. L. Wang, J. Majewski, E. Shavit, L. Leiserowitz and M. J. Lahav, Induced Freezing of Supercooled Water into Ice by Self-Assembled Crystalline Monolayers of Amphiphilic Alcohols at the Air-Water Interface, J. Am. Chem. Soc., 1994, 116, 1179–1191.
- 24 R. Heikkila, C. N. Kwong and D. G. Cornwell, Stability of fatty acid monolayers and the relationship between equilibrium spreading pressure, phase transformations, and polymorphic crystal forms, *J. Lipid Res.*, 1970, **11**, 190–194.
- 25 W. Lin, A. J. Clark and F. Paesani, Effects of Surface Pressure on the Properties of Langmuir Monolayers and Interfacial Water at the Air-Water Interface, *Langmuir*, 2015, 31, 2147–2156.
- 26 J. F. Davies, R. E. H. Miles, A. E. Haddrell and J. P. Reid, Influence of organic films on the evaporation and

- condensation of water in aerosol, *Proc. Natl. Acad. Sci. U. S. A.*, 2013, **110**(22), 8807–8812.
- 27 A. Heymsfield and P. Willis, Cloud Conditions Favoring Secondary Ice Particle Production in Tropical Maritime Convection, *J. Atmos. Sci.*, 2014, 71, 4500–4526.
- 28 K. V. Beard, Ice initiation in warm-base convective clouds: An assessment of microphysical mechanisms, *Atmos. Res.*, 1992, **28**, 125–152.
- 29 T. Zhang, M. G. Cathcart, A. S. Vidalis and H. C. Allen, Cation effects on phosphatidic acid monolayers at various pH conditions, *Chem. Phys. Lipids*, 2016, 200, 24–31.
- 30 W. D. Garrrett, The Organic Chemical Composition of the Ocean Surface, *U.S. Naval Res. Lab. Rept. 6201*, Dec. 24, Washington, D.C., 1964, p. 12.
- 31 N. L. Jarvis, W. D. Garrett, M. A. Scheiman and C. O. Timmons, Surface Chemical Characterization of Surface-active Material in Seawater, *Limnol. Oceanogr.*, 1967, 12, 88–96.
- 32 R. B. Gagosian, O. C. Zafiriou, E. T. Peltzer and J. B. Alford, Lipids in Aerosols from the Tropical North Pacific: Temporal variability, *J. Geophys. Res., C: Oceans Atmos.*, 1982, 87(C13), 11133–11144.
- 33 J. K. Schneider and R. B. Gagosian, Particle Size Distribution of Lipids in Aerosols off the Coast of Peru, *J. Geophys. Res., D: Atmos.*, 1985, **90**(D5), 7889–7898.
- 34 R. Iannone, D. I. Chernoff, A. Pringle, S. T. Martin and A. K. Bertram, The ice nucleation ability of one of the most abundant types of fungal spores found in the atmosphere, *Atmos. Chem. Phys.*, 2011, 11, 1191–1201, DOI: 10.5194/acp-11-1191-2011.
- 35 R. H. Mason, C. Chou, C. S. McCluskey, E. J. T. Levin, C. L. Schiller, T. C. J. Hill, J. A. Huffman, P. J. DeMott and A. K. Bertram, The micro-orifice uniform deposit impactor-droplet freezing technique (MOUDI-DFT) for measuring concentrations of ice nucleating particles as a function of size: improvements and initial validation, *Atmos. Meas. Tech.*, 2015, 8, 2449–2462.
- 36 N. S. Hiranuma, S. Augustin-Bauditz, H. Bingemer, C. Budke, J. Curtius, A. Danielczok, K. Diehl, K. Dreischmeier, M. Ebert, F. Frank, N. Hoffmann, K. Kandler, A. Kiselev, T. Koop, T. Leisner, O. Möhler, B. Nillius, A. Peckhaus, D. Rose, S. Weinbruch, H. Wex, Y. Boose, P. J. DeMott, J. D. Hader, T. C. J. Hill, Z. A. Kanji, G. Kulkarni, E. J. T. Levin, C. S. McCluskey, M. Murakami, B. J. Murray, D. Niedermeier, M. D. Petters, D. O'Sullivan, A. Saito, G. P. Schill, T. Tajiri, M. A. Tolbert, A. Welti, T. F. Whale, T. P. Wright and K. Yamashita, A comprehensive laboratory study on the immersion freezing behavior of illite NX particles: a comparison of 17 ice nucleation measurement techniques, *Atmos. Chem. Phys.*, 2015, 15, 2489–2518.
- 37 T. C. J. Hill, P. J. DeMott, Y. Tobo, J. Fröhlich-Nowoisky, B. F. Moffett, G. D. Franc and S. M. Kreidenweis, Sources of organic ice nucleating particles in soils, *Atmos. Chem. Phys.*, 2016, 16, 7195–7211, DOI: 10.5194/acp-2016-1.

- 38 Y. Tobo, An improved approach for measuring immersion freezing in large droplets over a wide temperature range, *Sci. Rep.*, 2016, **6**, 32930, DOI: 10.1038/srep32930.
- 39 P. J. DeMott, A. J. Prenni, G. R. McMeeking, Y. Tobo, R. C. Sullivan, M. D. Petters, M. Niemand, O. Möhler and S. M. Kreidenweis, Integrating laboratory and field data to quantify the immersion freezing ice nucleation activity of mineral dust particles, *Atmos. Chem. Phys.*, 2015, 15, 393– 409.
- 40 G. P. Schill, S. H. Jathar, J. K. Kodros, E. J. T. Levin, A. M. Galang, B. Friedman, D. K. Farmer, J. R. Pierce, S. M. Kreidenweis and P. J. DeMott, Ice nucleating particle emissions from photo-chemically-aged diesel and biodiesel

- exhaust, *Geophys. Res. Lett.*, 2016, **43**, 5524–5531, DOI: 10.1002/2016GL069529.
- 41 L. H. Seeley and G. T. Seidler, Preactivation in the nucleation of ice by Langmuir films of aliphatic alcohols, *J. Chem. Phys.*, 2001, **114**(23), 10464–10470, DOI: 10.1063/1.1375151.
- 42 B. Zobrist, T. Koop, B. P. Luo, C. Marcolli and T. Peter, Heterogeneous Ice Nucleation Rate Coefficient of Water Droplets Coated by a Nonadecanol Monolayer, *J. Phys. Chem. C*, 2007, **111**, 2149–2155, DOI: 10.1021/jp066080w.
- 43 J. R. Kanicky and D. O. Shah, Effect of Degree, Type, and Position of Unsaturation on the pK_a of Long-Chain Fatty Acids, *J. Colloid Interface Sci.*, 2002, **256**, 201–207, DOI: 10.1006/jcis.2001.8009.